



Optimized ANN-Based Methodology for Fault Detection and Localization in Power Transmission Networks

Adejumo Wahid Tunde ^{a*}, Emmanuel M. Eronu ^a
and Babawale B. Folajinmi ^a

^a Department of Electrical, Electronic Engineering, Faculty of Engineering,
University of Abuja, Nigeria.

Authors' contributions

This work was carried out in collaboration among all authors. Author AWT designed the study, performed the statistical analysis, wrote the protocol, and wrote the first draft of the manuscript. Authors EME and BBF managed the analyses of the study. Author BBF managed the literature searches. All authors read and approved the final manuscript.

Article Information

DOI: <https://doi.org/10.9734/jerr/2025/v27i11374>

Open Peer Review History:

This journal follows the Advanced Open Peer Review policy. Identity of the Reviewers, Editor(s) and additional Reviewers, peer review comments, different versions of the manuscript, comments of the editors, etc are available here: <https://www.sdiarticle5.com/review-history/129339>

Original Research Article

Received: 02/11/2024
Accepted: 04/01/2025
Published: 10/01/2025

ABSTRACT

Transmission lines are integral to transporting electrical power from generation sites to consumers. Transmission lines are subject to various faults that disrupt service and threaten system integrity. Fault analysis (identification, classification, and localization) is essential to minimize downtime and operational costs. Improved fault control raises grid dependability, decreases outages, and optimizes operations, promoting renewable integration and cost savings. It enhances safety, power quality, and resilience while facilitating innovative grid modernization and scalability for future demands. Such developments strengthen consumer trust and lead to more sustainable, efficient,

*Corresponding author: Email: tunad123@gmail.com;

and resilient power systems. This research employs Artificial Neural Networks (ANN) to enhance fault detection on high-voltage transmission lines. Simulations were conducted on a 132 kV, 50 Hz, 100 km transmission line model using MATLAB/Simulink, generating data from various fault scenarios. The ANNs, trained with these datasets, effectively and accurately analyzed the faults. The most effective neural network architecture was identified, assuring dependable operation in various fault scenarios and showcasing a strong strategy to enhance power transmission efficiency. Configuration 2 achieved the best fault identification accuracy of 97.99%, demonstrating the system's low error rate in accurately detecting the flaw. Fault classification with Configuration 1 attained a 95.65% accuracy rate. This indicates that the system can effectively categorize various fault types. The fault location was at an accuracy of 94.51% using Configuration 1.

Keywords: Fault identification; transmission line; artificial neural network; system reliability; fault localization.

1. INTRODUCTION

The ability of electrical power networks to supply electricity to industrial, commercial, and residential customers makes them essential to modern life. Relative turmoil, financial losses, and even fatalities may result from a brief power outage (Hines et al., 2009; GeneratorSource, n.d.). Power outages also impact a wide range of departments and organizations, some of which are deemed critical: those that depend on a steady supply of energy, such as the fire, police, and military departments, as well as hospitals, clinics, and health care facilities (Hachem-Vermette & Yadav, 2023). To keep the power system operating regularly after a transmission line breakdown, it is critical to promptly and accurately identify the fault source and address it (Liu, 2021; Saha & Izykowski, 2010). Ensuring faults are accurately detected and localized improves power transmission networks' dependability (Khan, 2024).

Apart from the significant financial implications, namely the time and money that can be saved during the fault detection process, pinpointing the precise location of the fault and quickly isolating the affected power section also improve the line's security against theft.

An electric power system made up of numerous intricately interacting components is always susceptible to disruptions or faults (Ranjithkumar et al., 2022). The world power system has grown significantly over the past few decades, necessitating the construction of many additional transmission and distribution lines. Because of this, the electrical power system must be brought back online as quickly as possible using maneuvers and corrective measures without compromising the reliability, quality, or continuity of the electric power supply (Adibi & Fink, 1994).

A power system fault is one of the most critical things preventing a steady power supply and electricity. A voltage and current divergence from their nominal values or states is referred to as an electrical fault (Almobasher & Habiballah, 2020). Regular operating conditions allow power system equipment or lines to carry regular voltages and currents, which makes system operation safer. Transmission line fault protection is the main focus of the majority of research conducted on the subject of protective relaying of power systems. Physically inspecting transmission lines for flaws might take several hours or a few minutes due to their length and ability to traverse different types of terrain (Babu et al., 2011). To locate these faults quickly, numerous utilities include fault-locating devices in their power quality monitoring systems (Paithankar & Bhide, 2012) outfitted with Global Information Systems. There are different categories for fault location techniques based on how many terminals are considered when gathering data.

However, the properties of subterranean cables and overhead lines (capacitance, inductance, resistance, etc.) differ significantly. On a hybrid transmission line, conventional protection devices (such as distance relays) are unable to recognize defects and pinpoint their positions with accuracy (Dasgupta et al., 2012). With a focus on neural networks, fuzzy logic, and evolutionary algorithms, an overview of popular techniques based on the artificial intelligence approach is given (Karti, 2003). Artificial neural networks (ANN) are one of the available techniques widely employed in this research to find defects in electric power transmission lines. Unlike other artificial intelligence-based approaches, these ANN-based approaches do not require a knowledge base for fault location (Kasztenny et al., 2004).

In (Koley et al., 2015), a hybrid approach based on DWT and ANN is presented for a six-phase line fault locator, classifier, and detector using just single-end measured data. The DWT-acquired estimated voltage and current signal standard deviation coefficients are sent into the ANN to facilitate fault localization and classification.

The application of wavelet analysis with ANN for accurate classification was investigated in (Saini et al., 2016). The method uses the fault classifier's approximation coefficient energy. Faults are accurately classified by applying DWT to obtain approximation coefficients for fault current signals. The Matlab/Simulink environment was utilized, and the suggested system was examined.

For fault detection and defective phase recognition, the author in (Kapoor et al., 2020) applies the Fast Walsh-Hadamard transform (FWHT) to a three-phase transmission line (TPTL). The FWHT has been thoroughly studied using TPTL's MATLAB test model. The transducers connected to the TPTL's bus 1 provide the three-phase fault current readings to the FWH algorithm. The procedure for detecting faults is quite precise.

ANN and DWT are integrated in (Saleh & Salam, 2012) for fault location and classification. After features are extracted using the DWT, fault signals are sent into the ANN. The integrated method enhances the precision and dependability of transmission line problem diagnostics. It shows how machine learning and advanced signal-processing techniques work well together. The methodologies vary from model-based techniques to machine learning to hybrid methods, focusing on defect detection, localization, and classification in power transmission lines. While these works have underlined achievements, further work is still required for accuracy, scalability, and interaction with emerging technologies toward a more robust fault analysis.

(Jamil et al., 2015) This study uses feed-forward neural networks and back-propagation to identify and classify transmission line faults based on three-phase currents and voltages. The method displays efficiency and adaptability through extensive simulations with different parameters and hidden layers, with the potential to be used in power distribution networks.

(He et al., 2014) This provides a fault classification approach for extra high voltage

transmission lines based on a Rough Membership Neural Network (RMNN) classifier. The wavelet process reflects time-frequency and time-domain characteristics, whereas RMNN classifiers and the Back Propagation (BP) algorithm improve performance. Simulations show that the suggested method outperforms common BPNN in terms of digital protection speed, accuracy, and robustness. In this research, the fault location was not considered.

Many authors who have worked on related research on fault analysis on transmission lines have used various inputs to train the ANN. However, there has been inadequate emphasis on comparing these input sets to determine which configurations yield the highest accuracy and most efficient neural network performance. This study addresses this gap by comparing different input sets to select the optimal combination for accurate fault analysis and performance.

2. MATERIALS AND METHODS

Artificial neural networks are the basis of the methodology used to accomplish the goals of this work. These networks use the parameters and data collected from the Transmission Company of Nigeria (TCN) to model a transmission line using MATLAB/SIMULINK. The extracted features from SIMULINK fault current and voltage signals are inputs to artificial neural networks. The core approach entails comparing input sets for training ANNs to determine which provides the best accuracy to optimize neural network performance.

The Sim-Power-Systems toolbox in MATLAB/Simulink software version 2018a was used to model a three-phase, single circuit, 132kV, 50 HZ, and 100km transmission line power system. It comprises 3-phase voltage and current measurements, transmission line pi-network, and 3-phase load. Various combinations of variables like current and voltage signals, RMS values, and sequence components are used at the fundamental frequency. The ANNs use a back-propagation algorithm trained on simulated fault scenarios to differentiate between non-faulty and faulty cases, classify fault types, and accurately localize faults along power transmission lines.

Simulations were performed using MATLAB/Simulink on a sample three-phase power system. The three-phase fault in the

Simulink environment introduced faults for all types of faults at ten different locations, with five different values of fault resistance at a sampling rate of 6.4 kHz.

The three phases' RMS voltages, currents, and sequence components are measured. The RMS voltages and currents consist of the RMS line-to-line voltages/currents (V_{ab} , V_{bc} , V_{ca} , I_{ab} , I_{bc} , I_{ca} ,) and the RMS phase voltages/currents (I_a , I_b , I_c , V_a , V_b , V_c ,). The sequence components are the zero sequence currents (I_0), positive sequence currents (I_p), and negative sequence currents (I_n). Twelve quantities were used to select the best input combinations for the neural network. The values are I_a , I_b , I_c , V_a , V_b , V_c , V_{ab} , V_{bc} , V_{ca} , and I_n/I_p , I_0/I_p , and I_p/I_{load} . The negative and positive sequences currents (I_n/I_p) ratio distinguishes balanced and unbalanced faults. The ratio of zero sequence current to positive sequence currents (I_0/I_p) distinguishes ground faults from phase faults. The ratio of positive sequence current to load currents (I_p/I_{load}) distinguishes balanced faults from no-fault conditions.

Three combinations of the six inputs were made based on the twelve measured quantities, and the best combination was selected based on the trained ANN. Three sets of feature combinations, namely Configuration-1, Configuration-2, and Configuration-3, are utilized for training the ANN.

For Configuration -1, inputs were V_a , V_b , V_c , and I_a , I_b , and I_c . Configuration -2 are V_{ab} , V_{bc} , V_{ca} , and I_n/I_p , I_0/I_p , and I_p/I_{load} while in Configuration -3 are V_a , V_b , and V_c and I_n/I_p , I_0/I_p , and I_p/I_{load} .

To achieve the objective, different input sets for training ANNs were compared to determine which provides the best accuracy to optimize neural network performance.

3. RESULTS AND DISCUSSION

This section gives the findings from the ANN fault prediction for this research. This research utilizes a single ANN technique within the same ANN structure to predict fault analysis. By leveraging the neural network's capabilities, the model effectively combines these three critical aspects of fault analysis, offering a comprehensive solution for identifying, classifying, and locating faults in electrical systems.

The model was optimized by varying the number of neurons in the single hidden layer. Starting

with ten neurons, the count was incrementally increased to 15, 20 to 25, and finally to 30 neurons. Each neuron employed the hyperbolic tangent sigmoid transfer function.

The training uses the Levenberg-Marquardt algorithm, with the mean square error (MSE) as the performance metric, utilizing MATLAB's "trainlm" function. Three models of single ANN structures were developed, each incorporating variations in input data for training and differing numbers of neurons in the hidden layers. These models were trained and evaluated to determine how effectively different ANN architectures, with varying input data ranges, could predict fault identification, classification, and location.

The evaluation began after training all the ANN architectures and compiling the complete testing data set. Subsequently, this testing data was fed into the trained ANN structures, allowing each ANN to generate fault predictions. The results from the ANN outputs were then compared to the actual testing target fault data.

For each case, the ANN output predictions were scrutinized against the actual fault data, focusing on fault analysis. The accuracy of fault identification and location predictions was assessed by calculating the error difference based on the absolute error between the actual and predicted values. The absolute error was calculated for all ANN output predictions for each ANN structure created using the various available measurement configurations. The mean absolute error (MAE) was used to assess the model's performance for fault classifications. A lower MAE corresponds to a more accurate classification model.

$$\text{Absolute Error} = \text{Actual Value} - \text{Predicted Value}$$

$$\text{Mean Absolute Error} = \frac{1}{N} \sum_{i=1}^n (y_i - y_{ii}) \quad (\text{R-bloggers, 2021}) \quad (1)$$

N = Number of observations

y_i = for the observation.

y_{ii} = for the observation.

The performance of each ANN model was thoroughly evaluated, providing insights into the effectiveness of different ANN structures in accurately predicting fault scenarios. This thorough process reassured the validity of the evaluation, highlighting the strengths and potential areas for improvement in the ANN.

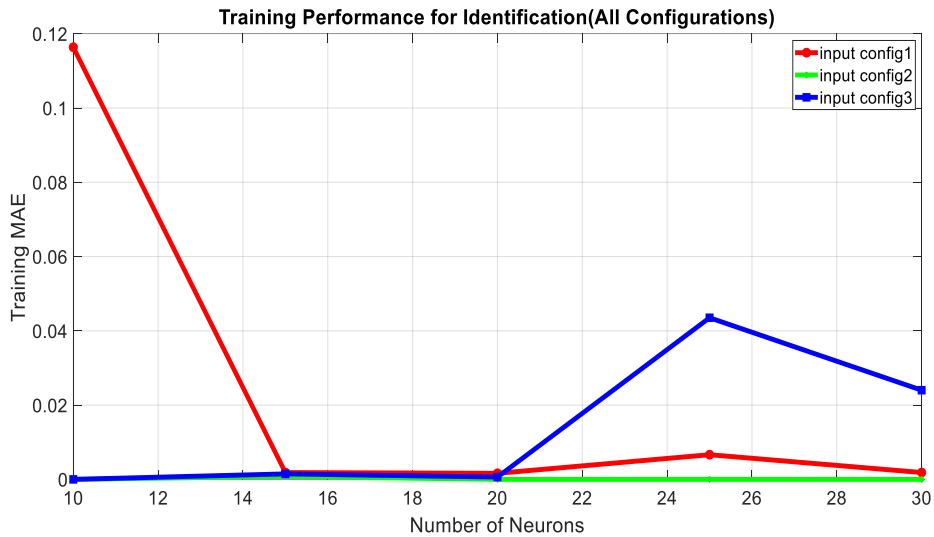


Fig. 1. Training Performance (MSE) for Fault Identification

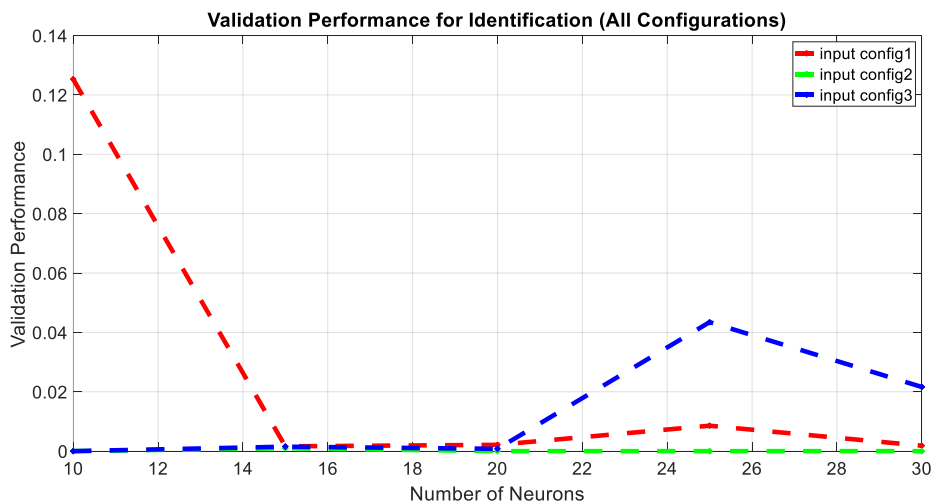


Fig. 2. Validation Performance (MSE) for fault identification

3.1 Training and Validation of Fault Identification for the Three Configurations

As shown in Fig. 1, Configuration 1 starts with 0.116364, portentously higher than the others, showing that the overall performance might be affected by this higher error. The preceding values exhibit a significant decrease, suggesting that the arrangement stabilizes at lower error rates with increased neurons. Configuration 2 continuously displays extremely low error levels, which suggests better training performance. Configuration 2 is the best overall training performance because it is steady and shows little fluctuations. Similar to configuration 2, configuration 3 begins with shallow error values

($3.76e-06$ and 0.001476), but as performance values (0.043523 and 0.024018) improve, they do so significantly.

The validation performance gives insights into how each configuration generalizes to unseen data after training. As shown in Fig. 2, Configuration 1 has validation performance values of 0.125292 , 0.001632 , 0.002131 , 0.008576 , and 0.001836 . The first value (0.125292) is relatively high compared to the others, indicating that the model may experience some difficulty in generalizing for certain validation sets. Configuration 2 displays low validation errors, with values close to zero in many instances. Configuration 3 starts with low error values ($4.96e-06$, 0.001512), but the error

increases significantly later (0.043454 and 0.021629). Configuration 3 shows some instability in certain validation sets, affecting its overall performance.

Configuration 2 points toward the best choice. It maintains the lowest error consistently during testing, validation, and training. Because the errors do not change significantly as the number of neurons increases, they can be generalized effectively and are less likely to over-fit. Because of its consistent overall performance, it is a good option for jobs involving identifying and locating faults in power transmission networks.

3.2 Training and Validation of Fault Classification for the Three Configurations

The values at ten and fifteen neurons, 0.004618 and 0.004102, respectively, are extremely low, as seen in Fig. 3, suggesting excellent learning with few errors employing Configuration 1. Yet, the value of 0.061546 is significantly higher at twenty neurons, indicating that the model had difficulty learning some parts of the fault classification during training.

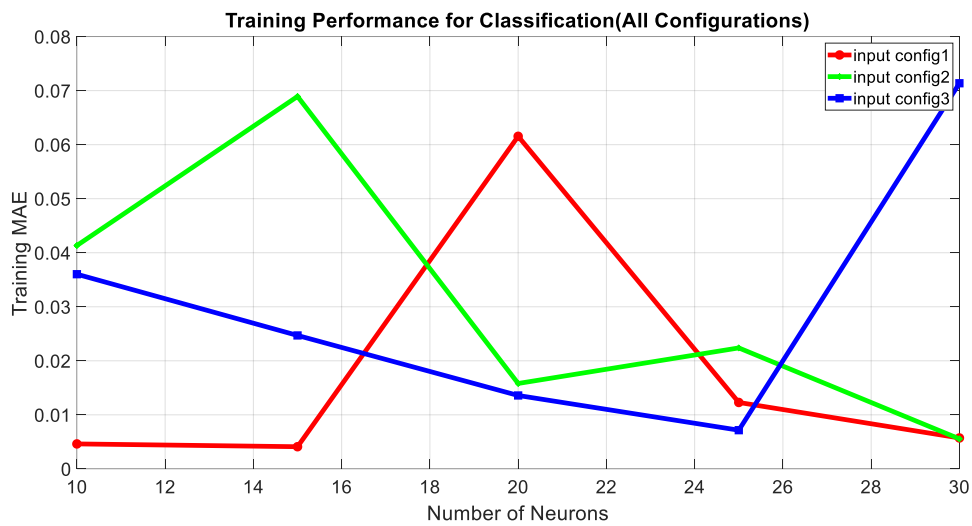


Fig. 3. Training Performance (MSE) for Fault Classification

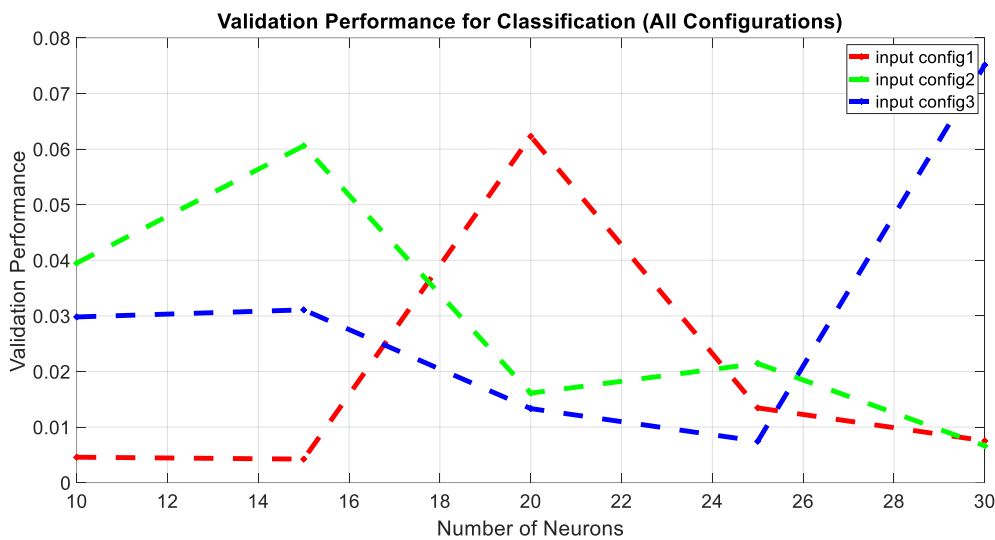


Fig. 4. Validation Performance (MSE) for Fault Classification

At ten and fifteen neurons, Configuration 2 has values (0.041335 and 0.068925) higher than those of Configuration 1. Additionally, Configuration 2 has more significant training errors, suggesting it might not be as effective as Configuration 1 during the training phase.

Configuration 3 has varied results, with some cases having errors as low as 0.013583 and others posing serious training challenges.

As shown in Fig. 4, Configuration 1 validation errors remain consistent, ranging between 0.0042 and 0.0623. Configuration 2 validation

errors are likewise high, indicating possible over-fitting, with a maximum error of 0.0606. The higher validation errors, approaching 0.0751, indicate over-fitting with Configuration 3.

Configuration 1 is the best choice due to its lower and more constant error rates during the training, validation, and testing phases for classification, despite a few significant errors. It provides a broader perspective that may be more applicable to fresh, previously unknown data. However, additional tuning may be required to solve specific high-error occurrences while improving overall efficiency.

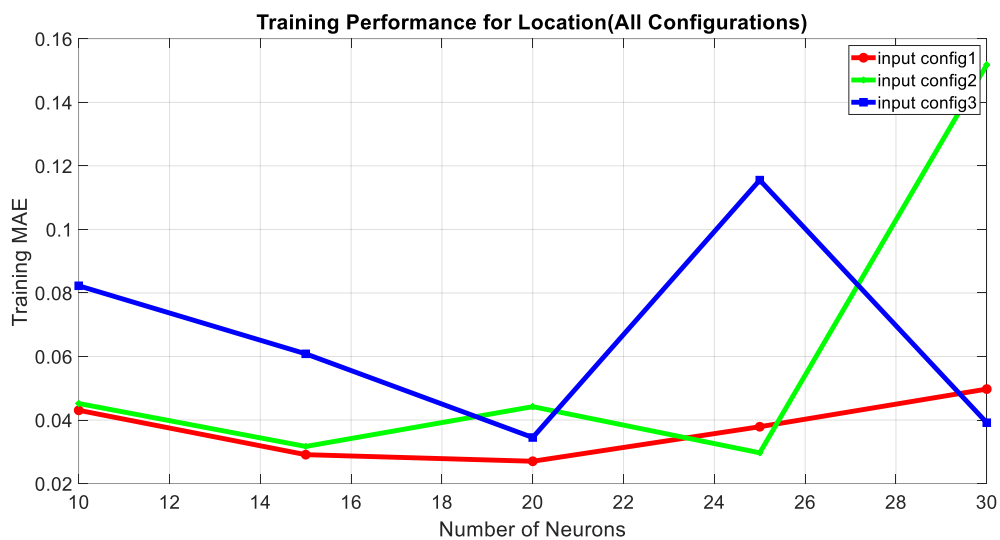


Fig. 5. Training Performance (MSE) for Fault Location

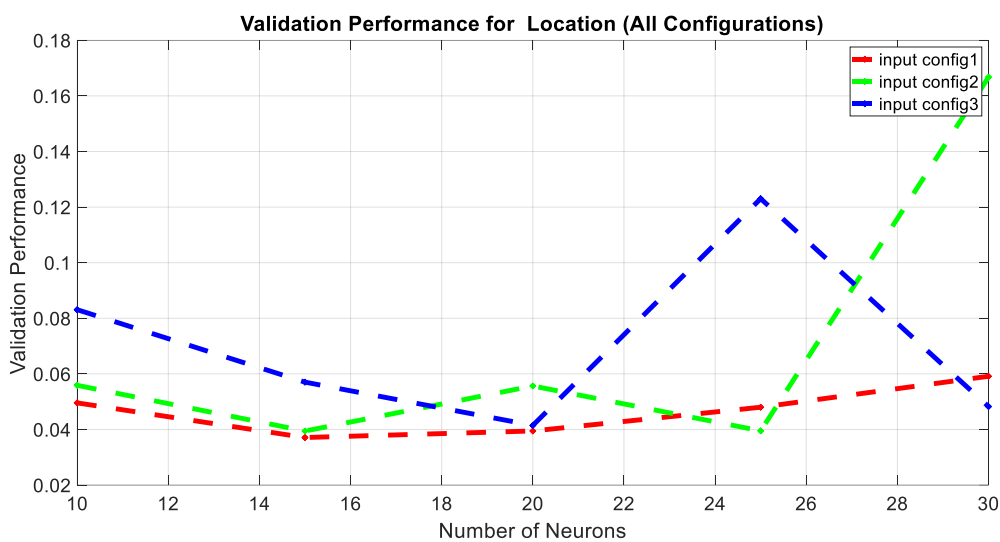


Fig. 6. Validation Performance (MSE) for Fault Location

3.3 Training, Validation and Test of Fault Location for the Three Configurations

Fig. 5 shows that Configuration 1 has the lowest and most consistent error rates across all phases. The errors are stable without noticeable spikes, showing strong generalization and robustness. Configuration 2 exhibits instability with large error spikes. Configuration 3 has higher and more variable errors.

Configuration 1 exhibits the best performance, with consistently low errors and steady behaviour across many instances, as seen in Fig. 6. Although Configuration 2 is generally good, the substantial inaccuracy of 0.16675 raises stability concerns. Of the three configurations, configuration 3 has the most significant errors and the lowest accuracy, indicating that it might not be the best choice for accurate fault location.

This indicates that Configuration 1 has the best possible option for fault location. It is more dependable, has better generalization, and shows less error variation throughout all stages.

3.4 Evaluation of Independent Data Performance for Fault Identification

Fig. 7 shows absolute errors in Configuration 1: 0.1099, 0.0258, 0.0225, 0.0319, and 0.0321. This combination's performance is average. The most significant error (0.1099) implies that there may be some occasions when the identification is not as accurate, but the rest are pretty modest, suggesting some consistency. However,

the difference between the greatest and lowest mistakes points to instability. Errors begin at 0.1099 (10 neurons) and decline progressively to 0.0225 (20 neurons), indicating better performance with more neurons. In contrast, errors increase slightly at 25 neurons (0.0319) and remain comparable at 30 neurons (0.0321). The absolute errors decrease as the number of neurons increases.

Configuration 2: 0.0194, 0.0346, 0.0088, 0.0200, and 0.0171 are the absolute errors. This configuration has the fewest overall errors, with most values falling between 0.01 and 0.03. The model's excellent ability to detect errors precisely is demonstrated by the lowest error of 0.0088. The small range of mistakes indicates better stability and generalization. It exhibits negligible errors in all neurons, with the lowest errors occurring in neurons 0.0195 (10 neurons) and 0.0088 (20 neurons) and the highest errors occurring at neurons 25 (0.0200) and 30 (0.0171). It maintains low errors throughout.

Configuration 3: Absolute Errors: 0.0823, 0.0608, 0.0345, 0.1155, 0.0392 Higher errors and more significant variation. The greatest error (0.1155) is the most important, which could indicate over-fitting or a struggle with classification accuracy for certain fault cases. The performance is more erratic, with the errors fluctuating significantly across different cases. The error values in this configuration are higher, rising at 0.1155 (25 neurons) and beginning at 0.0823 (10 neurons). As the number of neurons increases, noticeable variations point to instability.

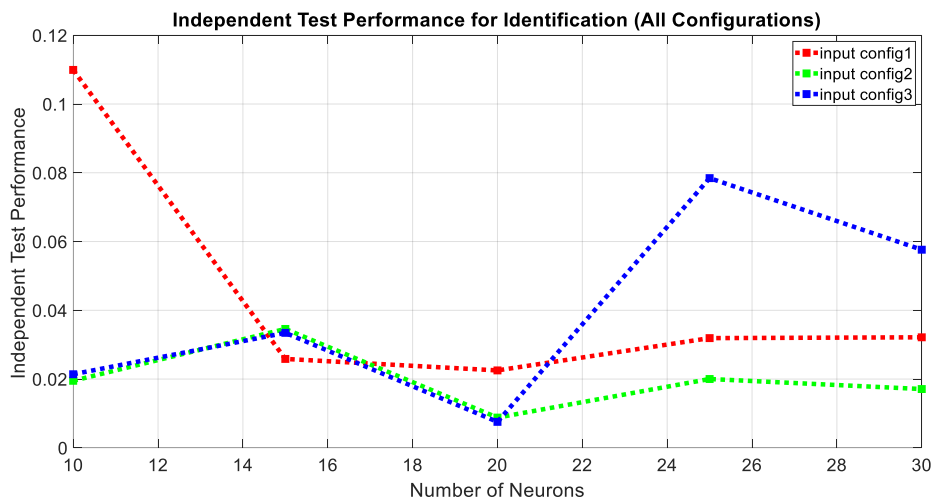


Fig. 7. Independent Performance (MSE) for Fault Identification

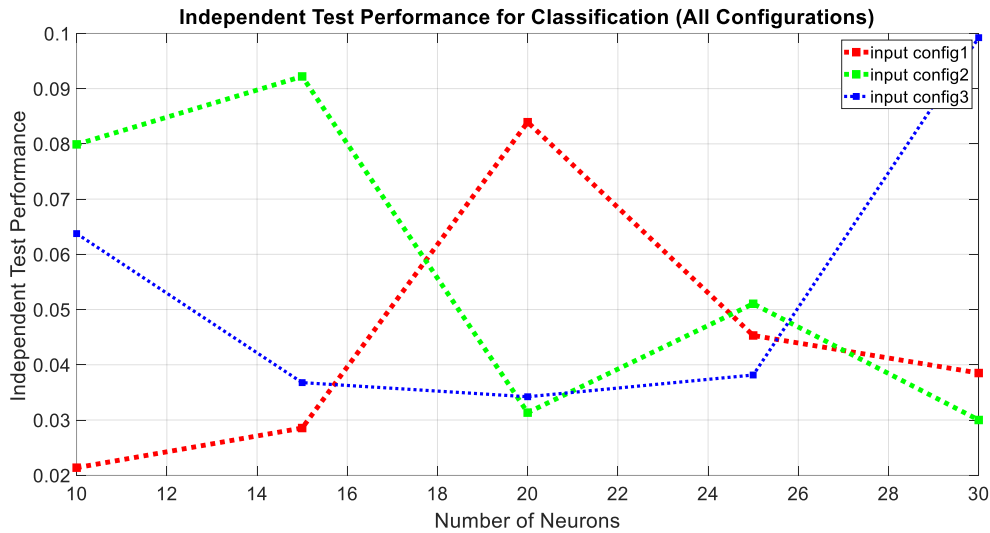


Fig. 8. Independent Performance (MSE) for Fault Classification

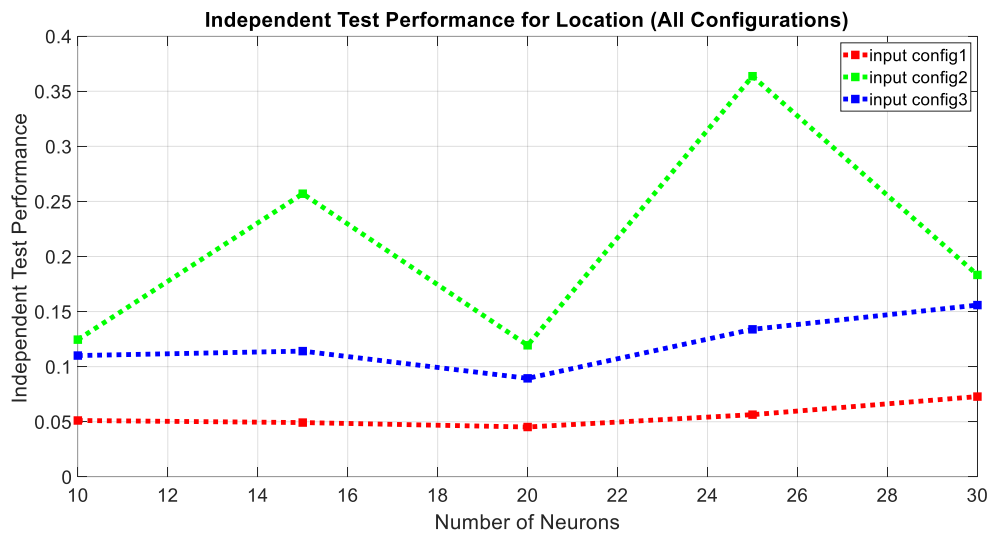


Fig. 9. Independent Performance (MSE) for Fault Location

For fault identification, Configuration 2, with 20 neurons, has the best independent test performance; it maintains the lowest errors overall and demonstrates better consistency and stability compared to Configurations 1 and 3. Configuration 1 shows moderate performance but with some instability, while Configuration 3 has higher and more varied errors, making it the least reliable.

3.5 Evaluation of Independent Data Performance for Fault Classification

Fig. 8 shows the MAE errors for Configuration 1 are 0.0214, 0.0285, 0.0839, 0.0453, and 0.0385. This setup displays a combination of moderate

and low mistakes. While the highest error (0.0839) indicates uneven performance or difficulties with particular fault types, the lowest error (0.0214) occasionally shows respectable performance. Overall, it shows adequate good performance with minor fluctuations. While errors increase with the number of neurons, they generally stay constant. Beginning at 0.0214 (10 neurons), the errors gradually increase until reaching a peak at 0.0839 (20 neurons). For increasing neuron counts, the errors stabilize between 0.0385 and 0.0453.

Configuration2 Mean Absolute errors include 0.0799, 0.0922, 0.0313, 0.0510, and 0.0300. It has substantially more mistakes than

Configuration 1, with the highest reaching 0.0922. This suggests poorer classification performance. Although a few errors (0.0300 and 0.0313) are moderate, the overall results indicate that this configuration fails to sustain low error levels across several circumstances. It begins with higher errors at 0.0799 (10 neurons) and 0.0922 (15 neurons), but at 20 neurons, with an error of 0.0313, it dramatically improves. This suggests that performance has improved thus far. For higher neurons, errors stabilize at 0.0510 and 0.0300.

Configuration 3 has the mean absolute errors of 0.0637, 0.0368, 0.0342, 0.0381, and 0.0992. It is more stable than Configuration 2, with shallow errors in most circumstances, except the most significant error of 0.0992. This spike at 0.0992 indicates instability or possibly over-fitting in some circumstances, but it performs marginally better than Configuration 2. Errors begin at 0.0637 (10 neurons) and decrease to 0.0342 (20 neurons) but are always moderate. At thirty neurons, it rises to 0.0992, indicating considerable instability.

Configuration 1 provides this analysis's most significant classification performance, with fewer errors and greater consistency across cases. While Configuration 3 does quite well, Configuration 1 has the fewest errors overall, making it the most dependable for fault classification. Configuration 2, on the other hand, produces more and less stable mistakes, making it the least desirable alternative.

3.6 Evaluation of Independent Data Performance for Fault location

Fig. 9 shows that Configuration 1 contains absolute errors of 0.0511, 0.0492, 0.0452, 0.0564, and 0.0728. It consistently produces low errors across all neuron configurations. The errors remain less than 0.073, showing good accuracy and stability in fault location performance. The error values increase slightly as the number of neurons increases, but they stay low and constant overall. Configuration 1 demonstrates good stability and accuracy in fault location tasks. The errors are continuously minimal, indicating that it can successfully handle fault locations across various neuron configurations. Errors vary from 0.0452 (20 neurons) to 0.0728 (30 neurons), which are consistently low and steady across all neuron counts. This exhibits the dependability and precision in fault location operations.

Configuration 2 has Absolute Errors of 0.1245, 0.2570, 0.1194, 0.3637, and 0.1833. This combination produces much increased errors, particularly with specific neurons. The errors significantly rise (0.2570, 0.3637), indicating low accuracy and instability in fault location tasks. The wide range in error magnitude suggests that this setup struggles to maintain accuracy as the network size changes. It shows significantly higher erratic errors, peaking at 0.3637 (25 neurons) and beginning at 0.1194 (10 neurons), indicating poor fault location performance.

Configuration 3 has absolute errors of 0.1101, 0.1141, 0.0894, 0.1339, and 0.1559. Configuration 3 contains more significant error numbers than Configuration 1, yet it outperforms Configuration 2. The errors are more constant but still in the higher range, reaching up to 0.1559 and indicating moderate performance with potential over-fitting in some neuron configurations. Compared to Configuration 2, errors are more excellent but consistent, ranging from 0.0894 (20 neurons) to 0.1559 (30 neurons). Because of this, Configuration 3 is less appropriate for precisely locating faults.

Configuration 1 is the most effective choice for fault location since it consistently produces the fewest and most stable faults across neuron configurations. Configurations 2 and 3 have greater error values, with Configuration 2 performing the worst due to huge error spikes. Thus, Configuration 1 is the most dependable for fault location tasks.

3.7 Percentage Accuracy for Identification, Classification, and Location

Assume that the accuracy is inversely proportional to the absolute inaccuracy and produce a % accuracy rating for each arrangement. The accuracy percentage can be obtained by applying the accompanying formula:

$$\text{Accuracy (\%)} = (1 - \text{Mean Absolute Error}) \times 100 \quad (2)$$

Assume the maximum possible error is 1 (100%).

Using the results from the independent test for identification, classification and location, the following values are obtained:

Table 1. Percentage Accuracy Obtained Across All the Configurations

Task	Configuration	Mean Absolute Error	Accuracy (%)
Identification	Configuration 1	0.04406	95.59%
	Configuration 2	0.02004	97.99%
	Configuration 3	0.06646	93.35%
Classification	Configuration 1	0.04352	95.65%
	Configuration 2	0.05688	94.31%
	Configuration 3	0.0544	94.56%
Location	Configuration 1	0.05494	94.51%
	Configuration 2	0.20958	79.04%
	Configuration 3	0.12068	87.93%

Table 2. Fault Identification Maximum and Minimum Error Comparison

Fault Type	Max. Mean Absolute Error	Distance (KM)	Fault Resistance (ohm)	Error %	Min. Mean Absolute Error	Distance (KM)	Fault Resistance (ohm)	Error %
AG	0.0176	20	1	2%	0.00099	80	0.5	0%
BG	0.01629	80	0.1	2%	0.00238	70	0.05	0%
CG	0.01867	80	1	2%	0.00013	70	0.05	0%
ABG	0.10593	10	1	11%	0.00002	30	0.05	0%
BCG	0.03749	10	0.05	4%	0.00459	10	0.1	0%
ACG	0.03562	30	0.1	4%	0.00315	10	0.5	0%
AB	0.05742	100	0.01	6%	0.00047	20	0.1	0%
BC	0.03651	10	0.05	4%	0.00383	80	0.1	0%
AC	0.03193	100	0.05	3%	0.00029	50	0.5	0%
ABC	0.02512	60	0.05	3%	0.00453	10	0.05	0%
NF	0.01047	20	1	0%	0.01151	60	0.5	1%

Table 3. Fault Classification Maximum and Minimum Error

Fault Type	Max. Mean Absolute Error	Distance (KM)	Fault Resistance (ohm)	Error %	Min. Mean Absolute Error	Distance (KM)	Fault Resistance (ohm)	Error %
AG	0.01974	10	0.01	2%	0.0023	20	0.05	0%
BG	0.00115	10	0.01	1%	0.00357	50	0.5	0%
CG	0.02458	20	0.01	2%	0.00088	80	1	0%
ABG	0.07327	20	1	7%	0.0027	30	0.01	0%
BCG	0.12479	20	0.1	12%	0.00505	30	0.05	0%
ACG	0.08366	10	0.1	8%	0.01316	20	1	1%
AB	0.08100	10	0.05	8%	0.00269	50	0.5	0%
BC	0.07016	20	0.05	7%	0.00407	20	0.01	0%
AC	0.05109	50	0.5	5%	0.0187	20	0.05	2%
ABC	0.03288	20	0.1	3%	0.000171	70	0.5	0%
NF	0.02548	100	0.01	3%	0.02436	20	0.01	0%

Table 4. Fault Location Maximum and Minimum Error

Fault Type	Max. Mean Absolute Error	Distance (KM)	Fault Resistance (ohm)	Error %	Min. Mean Absolute Error	Distance (KM)	Fault Resistance (ohm)	Error %
AG	12.186	80	0.5	12%	0.106	90	0.1	0.0%
BG	8.776	10	0.05	9%	0.035	70	0.1	0%
CG	7.045	20	0.1	7%	0.080	60	1	0%
ABG	12.291	30	0.01	12%	0.791	50	0.01	1%
BCG	11.518	30	0.05	12%	0.219	30	0.1	0%
ACG	7.101	30	1	7%	0.407	70	1	0%
AB	13.429	20	0.1	13%	1.417	80	1	1%
BC	11.991	20	0.05	12%	0.195	90	1	1%
AC	3.648	90	0.5	4%	0.398	50	1	0%
ABC	8,688	10	0.05	9%	0.266	50	0.1	0.0%

Table 1 shows the percentage accuracy of the faults analysis according to their different setups. The Mean Absolute Error (MAE) is used to calculate accuracy for each activity, and it is inversely related to accuracy, implying that lower error numbers equate to greater accuracy.

With an accuracy rate of about 98%, identification outperforms the other two jobs and is the most dependable in this Investigation. The best configuration for this work has been offered by Configuration 2. With over 95% accuracy, the classification task executes excellently by Configuration 1. While Configuration 1 performs strongly, it performs slightly lower than identification regarding fault class distinction. Also, fault location performance is excellent, with more than 94% accuracy. However, location accuracy is less accurate than identification and classification because it is more difficult to determine the precise location of the fault.

Table 2 compares the maximum and minimum mean absolute errors for different fault types during identification. It also gives the associated distances, fault resistances, and error percentages, showing how effectively each fault type is identified.

Fault types such as AG, BG, CG, ABC, and NF have minimal maximum and minimum errors of 0 and 3%, indicating accurate identification in these cases.

The ABG and AB faults have the highest maximum errors (11 percent and 6 percent, respectively), which shows that these fault types are more difficult to identify due to their complexity.

The errors across all fault types are often relatively low, indicating that the identification system functions well over a wide range of distances and fault resistance.

Table 3 compares the maximum and minimum mean absolute errors for several fault categories in fault classification. The corresponding error percentages, fault resistances, and associated distances are given for each fault type, providing information about the classification performance.

The best results are obtained at the maximum and minimum errors for fault types like AG, BG, CG, ABC, and NF, which are extremely small and fall between 1% and 3%. Certain fault types are accurately classified even at higher fault resistances and longer distances.

AB and BCG faults have the highest maximum errors (8% and 12%, respectively) regarding challenging defects. This error shows that the classification procedure for these fault types is more complex, leading to significantly less accurate performance when compared to other fault types. Inaccuracies were also related to longer lengths and lower resistances. The bulk of detected faults have extremely low error percentages, indicating that the system performs well across various fault types, resistances, and distances. The project will seek a solution to one of the most critical components of ensuring the reliability and efficiency of power transmission systems, i.e., precise fault detection. Precision fault detection contributes to power transmission networks' operational dependability and safety.

Table 4 compares the maximum and minimum mean absolute errors for various fault types and the accompanying fault resistances and distances. It also gives the error percentages related to every situation.

The AB and ABG faults had the highest errors, with maximum mean absolute errors of 13.429 (13%) and 12.291 (12%), respectively, occurring at shorter distances (20-30 KM) and low fault resistances (0.01-0.1 ohm). The error rates for BC and BCG faults are also noteworthy, with 11.991 (12%) and 11.518 (12%), respectively. The fact that these faults usually occur at low resistances suggests that locating them precisely in some situations may be challenging.

On the other hand, faults like AG, BG, and ABC have more fault resistance and produce fewer errors across greater distances. For example, the AG fault has a minimum error of 0.106 at 90 km and 0.1 ohm, but BG faults have an error of 0.035 at 70 km. Similarly, ABC defects have a low error of 0.266 at 50 km.

Short distances and lower faults result in more significant errors for most fault types, which could be attributed to fault resistance. However, high fault resistances with longer distances have high fault location accuracy. Faults such as AB, ABG, and BC present the most significant obstacles, but faults such as AG and BG exhibit higher precision in their location.

Lower fault resistances tend to raise the maximum error percentage, but higher fault resistances lead to lower minimum errors, most likely due to improved detection sensitivity under high-resistance conditions.

4. CONCLUSION

A detailed effort has been conducted on fault analysis on transmission lines utilizing neural networks, precisely the back-propagation method. The primary purpose is to find the best neural network configuration to ensure high accuracy and stability across different fault scenarios to detect, categorize, and locate faults in a 100-kilometer transmission line at 132kV and 50Hz frequency. This study evaluated three different ANN configurations with varying neuron counts for fault analysis on power transmission systems. Strong accuracy performance is shown for all tasks when the neural network models for the fault analysis are analyzed.

Using Configuration 2, fault identification attained a fantastic accuracy of 97.99%, demonstrating the system's ability to identify the fault with little error.

With Configuration 1, fault classification attained an accuracy of 95.65%. This shows that the system can successfully classify different kinds of faults, although with a little less accuracy than when it comes to identification. Even at the accuracy of 94.51% (Configuration 1), fault location is still performing at a high level. The accuracy of fault localization slightly decreased because finding a fault is frequently more complex than classifying or identifying it.

Configuration 1 achieves perfect fault classification and location results, while Configuration 2 excels in fault identification. This implies that specific configurations might be more appropriate for various jobs, depending on complexity and needs. The remarkable outcome in all three tasks demonstrates the approaches' potential to significantly improve transmission line operations' reliability, efficiency, and resilience.

DISCLAIMER (ARTIFICIAL INTELLIGENCE)

Author(s) hereby declare that NO generative AI technologies such as Large Language Models (ChatGPT, COPILOT, etc.) and text-to-image generators have been used during the writing or editing of this manuscript.

ACKNOWLEDGEMENTS

My sincere appreciation goes out to God Almighty for his kindness, protection, strength, intelligence, and wisdom during my academic

journey. This initiative has succeeded because of his engagement.

I want to thank my esteemed supervisors, Dr. E. M. Eronu and Dr. Alfa, for their assistance, guidance, and support throughout this project. Their dedication and encouragement have had a significant impact on the course of our research.

I am deeply indebted to my family, Alh. Rhodiat Akanbi, Dr. Jubril Akolade, Mr. Kaoyde Ogungbade, and others, for their steadfast belief in my aspirations, unceasing support, and uplifting encouragement. They have consistently been a wellspring of love and empathy, and I am profoundly grateful.

COMPETING INTERESTS

Authors have declared that no competing interests exist.

REFERENCES

- Adibi, M. M., & Fink, L. H. (1994). Power system restoration planning. *IEEE Transactions on Power Systems*, 9(1), 22–28. <https://doi.org/10.1109/59.295994>
- Almobasher, L., & Habiballah, I. (2020). Review of power system faults. *International Journal of Engineering and Technical Research*, 9, 61.
- Babu, S., et al. (2011). Fault location in power systems. *International Journal of Engineering, Science and Technology*, 2(3), 1-8.
- Dasgupta, A., et al. (2012). Transmission line fault classification and location using wavelet entropy and neural network. *Electric Power Components and Systems*.
- GeneratorSource. (n.d.). Causes of power failures. Retrieved from https://www.generatorsource.com/Causes_of_Power_Failures.aspx
- Hachem-Vermette, C., & Yadav, S. (2023). Impact of power interruption on buildings and neighborhoods and potential technical and design adaptation methods. *Sustainability*, 15(21), 15299. <https://doi.org/10.3390/su152115299>
- He, Z., Lin, S., Deng, Y., Li, X., & Qian, Q. (2014). A rough membership neural network approach for fault classification in transmission lines. *International Journal of Electrical Power & Energy Systems*, 61, 429-439. <https://doi.org/10.1016/j.ijepes.2014.04.014>

- Hines, P., Apt, J., & Talukdar, S. (2009). Large blackouts in North America: Historical trends and policy implications. *Energy Policy*, 37(12), 5249-5259. <https://doi.org/10.1016/j.enpol.2009.07.010>
- Jamil, M., Sharma, S. K., & Singh, R. (2015). Fault detection and classification in electrical power transmission system using artificial neural network. *SpringerPlus*, 4, 1-3. <https://doi.org/10.1186/s40064-015-0957-7>
- Kapoor, G., Soni, V., & Yadvendra, J. (2020). Fast Walsh–Hadamard transform-based artificial intelligent technique for transmission line fault detection and faulty phase recognition. In *Proceedings of the International Conference on Artificial Intelligence: Advances and Applications 2019* (pp. 141-149). Springer Singapore.
- Kasztenny, B., Voloh, I., & Hubertus, J. G. (2004, April). Applying distance protection to cable circuits. In *Proceedings of the 57th Annual Conference for Protective Relay Engineers* (pp. 46-69). IEEE.
- Khan, M. (2024). Investigating the effects of ageing on transmission system dependability through the use of an artificial neural network. *Journal of Electrical Systems*, 20, 1059-1066. <https://doi.org/10.52783/jes.2838>
- Koley, E., Verma, K., & Ghosh, S. (2015). An improved fault detection, classification, and location scheme based on wavelet transform and artificial neural network for six-phase transmission line using single-end data only. *SpringerPlus*, 4(1), 1-22. <https://doi.org/10.1186/s40064-015-0963-9>
- Krarti, M. (2003). *Solar energy engineering: Processes and systems*. *Journal of Solar Energy Engineering*, 125(3), 331-342. <https://doi.org/10.1115/1.1577052>
- Liu, X. W. (2021). Research on transmission line fault location based on the fusion of machine learning and artificial intelligence. *Security and Communication Networks*, 2021, Article ID 6648257, 8 pages. <https://doi.org/10.1155/2021/6648257>
- Paithankar, Y. G., & Bhide, S. R. (2012). *Fundamentals of power system protection*. PHI Learning.
- Ranjithkumar, K., Kumar, N. R. N., Nishanth, S., Anand, A. S. S., & Priyanka, S. (2022). Distribution fault identification and protection using LabVIEW. In *Proceedings of the 2022 International Conference on Computer Communication and Informatics (ICCCI)*, Coimbatore, India, 1-3. <https://doi.org/10.1109/ICCCI54379.2022.9741013>
- R-bloggers. (2021, July). How to calculate mean absolute error in R. Retrieved from <https://www.r-bloggers.com/2021/07/how-to-calculate-mean-absolute-error-in-r/>
- Saha, M. M., & Izykowski, E. (2010). *Fault location on power networks*. Springer-Verlag London Limited.
- Saini, M., bin Mohd Zin, A. A., bin Mustafa, M. W., Sultan, A. R., & Rahimuddin, M. (2016). Transmission line fault detection using discrete wavelet transform and back-propagation neural network based on Clarke's transformation. *Applied Mechanics and Materials*, 818, 156–165. <https://doi.org/10.4028/www.scientific.net/AMM.818.156>
- Saleh, S. A., & Salam, M. A. (2012). Transmission line fault detection and classification using discrete wavelet transform and artificial neural network. *Journal of Electrical Engineering and Technology*, 7(4), 409-417. <https://doi.org/10.5370/JEET.2012.7.4.409>

Disclaimer/Publisher's Note: The statements, opinions and data contained in all publications are solely those of the individual author(s) and contributor(s) and not of the publisher and/or the editor(s). This publisher and/or the editor(s) disclaim responsibility for any injury to people or property resulting from any ideas, methods, instructions or products referred to in the content.

© Copyright (2025): Author(s). The licensee is the journal publisher. This is an Open Access article distributed under the terms of the Creative Commons Attribution License (<http://creativecommons.org/licenses/by/4.0>), which permits unrestricted use, distribution, and reproduction in any medium, provided the original work is properly cited.

Peer-review history:

The peer review history for this paper can be accessed here:

<https://www.sdiarticle5.com/review-history/129339>